Available online at www.sciencedirect.com
ScienceDirect
Mechanics of Materials 39 (2007) 94–103
MECHANICS OF MATERIALS
www.elsevier.com/locate/mechmat

A unified scheme for prediction of effective moduli of multiphase composites with interface effects: Part II—Application and scaling laws

H.L. Duan, X. Yi, Z.P. Huang, J. Wang *

LTCS and Department of Mechanics and Engineering Science, Peking University, Beijing 100871, PR China

Received 6 February 2006; received in revised form 6 February 2006

Abstract

In this part, first, the detailed expressions for the effective moduli of multiphase composites containing spherical particles or fibres are presented following the theoretical framework developed in Part I. Second, the effect of the interfacial bonding conditions on the effective moduli of these composites are examined. It is shown that the imperfect bonding condition can considerably affect the effective moduli of the composites. Third, as the effective moduli of the composites with the considered linear-spring and interface stress effects become dependent upon the size of the particles or fibres, two simple scaling laws are derived to depict the size-dependence. It is shown that whilst the interface effects simulated by the two interface models are opposite from a physical point of view, the scaling laws for them are formally reciprocal from a mathematical one.

Keywords: Multiphase composites; Effective moduli; Interface effects; Linear-spring model; Interface stress model; Interphase model; Size-dependence; Scaling laws

1. Introduction

The macroscopic properties of multiphase composites depend upon the properties and the interfacial bonding conditions of the constituent phases, and the microstructures of the composites. Thus the effect of the interfacial bonding conditions on the mechanical and physical properties of various composites has attracted a lot of attention of researchers in many fields, especially, in physics, materials science and technology, and mechanics. The prediction of the effective moduli taking into account various interface effects is one of the fundamental problems in mechanics of composites. Simple and accurate micromechanical schemes for predicting the effective moduli have been constantly pursued. In the first part of this two-part paper, we have presented a replacement procedure that transforms spherical particles and cylindrical fibres with the three kinds of interface effect into equivalent homogeneous particles and fibres. The moduli of these equivalent particles and fibres have also been given. These equivalent reinforcements are then

* Corresponding author. Tel.: +86 10 6275 7948.
E-mail address: jxwang@pku.edu.cn (J. Wang).

0167-6636/$ - see front matter © 2005 Published by Elsevier Ltd.
doi:10.1016/j.mechmat.2006.02.010

embedded in, and regarded as being perfectly bonded to, the matrix materials of the respective composites. Thus, various micromechanical schemes for multiphase composites can be readily used to predict the effective moduli of the concerned composites using the elastic constants of the matrix materials and the equivalent reinforcements. For the reasons shown in Part I, in this paper, we choose to use the generalized self-consistent method (GSCM) to predict the effective moduli of the composites. However, unlike the classical GSCM (Christensen and Lo, 1979), we have proposed to calculate the stress (strain) concentration tensors using the Eshelby equivalent inclusion method in an average sense. As will be shown in detail, this modified generalized self-consistent method (Duan et al., 2006) gives much simpler expressions of the effective shear moduli than the classical GSCM. In this part, the framework developed in Part I will be applied to particle- or fibre-reinforced composites with the interface effects. Examples will be given to demonstrate the details of the application of the scheme and the influence of the interface effects on the effective moduli of the composites.

This part is organized as follows. In Section 2, we shall give the detailed expressions of the effective moduli of particle- or fibre-reinforced two-phase composites derived using the modified generalized self-consistent method. This scheme will be compared with the classical GSCM to verify its accuracy. In Section 3, the GSCM predictions will be incorporated into the decoupled formulas to calculate the effective moduli of composites containing multiple kinds of particle or fibre. In Section 4, the effective moduli of multiphase composites with the interface effects will be examined in detail using the developed scheme in this paper. In Section 5, two kinds of simple scaling law depicting the size-dependence of the effective moduli corresponding to the linear-spring model and interface stress model are given. Finally, some conclusions are drawn in Section 6.

2. Effective moduli of two-phase composites

As indicated in Part I, the spherical particles and cylindrical fibres with the three kinds of interface effect can be replaced by the corresponding equivalent particles and fibres, which are in turn perfectly bonded to the matrix materials. The interface effects are taken into account in the moduli of the equivalent particles and fibres. Thus, in this section and the next, we shall simply discuss the prediction of the effective moduli of particle- or fibre-reinforced composites with perfect interfacial bonding conditions.

2.1. Particle-reinforced composites

Here, we consider a two-phase composite which is composed of a continuous matrix and randomly distributed spherical particles of the same stiffness. For this composite, we reproduce the expressions for the effective moduli obtained by Duan et al. (2006). When substituting $\overline{\mathbf{T}}^*$ in Eq. (I48) into Eq. (I43) (In this part, formulas from Part I are distinguished by the prefix I.), it is found that the obtained effective bulk modulus $\bar{\kappa}$ is identical to that given by the classical GSCM (Christensen and Lo, 1979), and the MTM (Mori and Tanaka, 1973; Benveniste, 1987), i.e.

$$\bar{\kappa} = \frac{4(1-f_I)\kappa_1\mu_1 + \kappa_I(3\kappa_1 + 4f_I\mu_1)}{3(1-f_I)\kappa_I + 3f\kappa_1 + 4\mu_1} \tag{1}$$

where κ_1 and μ_1 are the bulk and shear moduli of the matrix, κ_I and μ_I are those of the particles, and f_I is the volume fraction of the particles. The effective shear modulus, denoted by $\bar{\mu}$, needs to be solved from the following quadratic equation in $\bar{\mu}/\mu_1$ (Duan et al., 2006):

$$A'\left(\frac{\bar{\mu}}{\mu_1}\right)^2 + B'\left(\frac{\bar{\mu}}{\mu_1}\right) + C' = 0 \tag{2}$$

where

$$\begin{aligned} A' &= -[126f_I^{7/3} - 252f_I^{5/3} + 50(7 - 12\nu_1 + 8\nu_1^2)f_I] \\ &\quad \times (1 - g_3) + 4(7 - 10\nu_1)N \\ B' &= [252f_I^{7/3} - 504f_I^{5/3} + 150(3 - \nu_1)\nu_1 f_I] \\ &\quad \times (1 - g_3) - 3(7 - 15\nu_1)N \\ C' &= -[126f_I^{7/3} - 252f_I^{5/3} + 25(7 - \nu_1^2)f_I] \\ &\quad \times (1 - g_3) - (7 + 5\nu_1)N \end{aligned} \tag{3}$$

in which $N = -7 + 5\nu_1 - 2g_3(4 - 5\nu_1)$, $g_3 = \mu_\mathrm{I}/\mu_1$ and ν_1 is the Poisson ratio of the matrix. It is seen that the coefficients A', B' and C' are much simpler than their counterparts in the classical GSCM. It has been demonstrated that the effective shear modulus given in Eq. (2) is numerically indistinguishable from the classical GSCM for various composites (Duan et al., 2006).

2.2. Fibre-reinforced composites

Here, we consider a composite consisting of a continuous matrix and aligned but randomly

distributed cylindrical fibres of the same stiffness. Such a composite is a macroscopically transversely isotropic material which has five independent elastic constants. Among the five elastic constants, those related to the longitudinal (fibre) direction and the plane-strain bulk modulus in the plane perpendicular to the fibres can be easily and accurately predicted by the composite cylinder model of Hill (1964), and Hashin (1966). The prediction of the transverse shear modulus poses a problem for the composite cylinder model, although the model can give bounds on the shear modulus. Christensen and Lo (1979) developed the generalized self-consistent method to calculate the transverse shear modulus. The configuration of the model is shown in Fig. 2(a) in Part I, which should be understood in a two-dimensional sense. Therefore, when the theoretical framework developed in Part I is applied in a two-dimensional sense, we can calculate the effective transverse plane-strain bulk modulus and the transverse shear modulus of the aligned fibre-reinforced composite. Similar to the case for the spherical particle, when substituting $\overline{\mathbf{T}}^*$ in Eq. (I48) into Eq. (I43), it is found that the obtained effective plane-strain bulk modulus $\bar{k}$ is identical to that given by the classical GSCM (Christensen and Lo, 1979), i.e.

$$\bar{k} = \frac{(1-f_I)k_1\mu_1 + k_I(k_1+f_I\mu_1)}{(1-f_I)k_I + f_Ik_1 + \mu_1} \tag{4}$$

where k_1 and μ_1 are the plane-strain bulk and shear moduli of the matrix, respectively, k_{I} is the plane-strain bulk modulus of the fibres, and f_{I} denotes the volume fraction of the fibres. The effective transverse shear modulus of the composite, denoted by $\bar{\mu}_{\mathrm{T}}$, needs to be solved from the following quadratic equation in $\bar{\mu}_{\mathrm{T}}/\mu_1$:

$$a'\left(\frac{\bar{\mu}_{\mathrm{T}}}{\mu_1}\right)^2 + b'\left(\frac{\bar{\mu}_{\mathrm{T}}}{\mu_1}\right) + c' = 0 \tag{5}$$

where

$$\begin{aligned} a' &= [-3f_I^3 + 6f_I^2 - 4(4\nu_1^2 - 6\nu_1 + 3)f_I] \\ &\quad \times (1-g_2) - (3-4\nu_1)N_1 \\ b' &= [6f_I^3 - 12f_I^2 + 8\nu_1 f_I](1-g_2) + 2(1-2\nu_1)N_1 \\ c' &= [-3f_I^3 + 6f_I^2 - 4f_I](1-g_2) + N_1 \end{aligned} \tag{6}$$

with $N_1 = 1 + g_2(3-4\nu_1)$, $g_2 = \mu_{\mathrm{T}I}/\mu_1$, $\mu_{\mathrm{T}I}$ is the transverse shear modulus of the fibres, and ν_1 is the Poisson ratio of the matrix. Again, it is seen that the coefficients a', b' and c' are much simpler than their counterparts in the classical GSCM. Similarly, it can be demonstrated that the effective transverse shear modulus given in Eq. (5) is numerically indistinguishable from the classical GSCM for various composites; the detailed numerical results are omitted for brevity.

3. Effective moduli of multiphase composites

3.1. Particle-reinforced composites

As pointed out in Section 4.3 in Part I, the effective moduli of multiphase composites can be calculated using Eq. (I43) or (I44) together with the stress or strain concentration tensors calculated in Eq. (I48) or (I51) for each kind of particle. However, for multiphase composites, either Eq. (I43) or (I44) results in two coupled nonlinear equations with the effective moduli being the unknowns. Thus it is not very convenient to calculate the effective moduli. To circumvent this difficulty while still taking advantage of the accuracy of the generalized self-consistent method, Huang et al. (1994) proposed a decoupled method to calculate the effective moduli of multiphase composites using the results of the GSCM. This method is implemented as follows. For a general multiphase composite with $N-1$ kinds of particle, denoted by $I = 2, \ldots, N$, the normalized effective moduli of the composite can be calculated with high accuracy by the following decoupled formulas:

$$\frac{\bar{\kappa}}{\kappa_1} \cong \prod_{I=2}^{N} \frac{\bar{\kappa}_0}{\kappa_1}\left(f_I, \frac{\mu_I}{\mu_1}, \nu_I, \nu_1\right) \tag{7}$$

$$\frac{\bar{\mu}}{\mu_1} \cong \prod_{I=2}^{N} \frac{\bar{\mu}_0}{\mu_1}\left(f_I, \frac{\mu_I}{\mu_1}, \nu_I, \nu_1\right) \tag{8}$$

where $\bar{\kappa}_0(f_I, \mu_I/\mu_1, \nu_I, \nu_1)$ and $\bar{\mu}_0(f_I, \mu_I/\mu_1, \nu_I, \nu_1)$ are the effective bulk and shear moduli of the two-phase composite that comprises the matrix material of the considered multiphase composite and the I-th kind of particle.

Huang et al. (1994) calculated the effective bulk and shear moduli of multiphase particle-reinforced composites using Eqs. (7) and (8), along with the bulk and shear moduli of two-phase composites of Christensen and Lo (1979). In this paper, we calculate the effective moduli of multiphase particle-reinforced composites using Eqs. (7) and (8), along with Eqs. (1) and (2). Our numerical results also show that the decoupled formulas in Eqs. (7) and (8) are

very accurate compared with the detailed numerical results computed from the coupled nonlinear algebraic equations (I43) or (I44). It has been shown that for two-phase composites, Eqs. (I43) and (I44), together with the respective stress and strain concentration tensors in (I48) and (I51), give the identical effective moduli, which means that the present method is indeed self-consistent. In the following, the numerical results of the effective moduli obtained from the solution of the nonlinear equations in Eqs. (I43) or (I44) will be compared with Eqs. (7) and (8) to show the accuracy of the latter.

Fig. 1(a) shows the variation of the effective Young modulus of a composite comprising a matrix of epoxy, quartz-sand particles (second phase) and voids (third phase) studied by Cohen and Ishai (1967). The material parameters are: $E_1 = 2.03$ GPa, $\nu_1 = 0.4$, $E_2 = 73.6$ GPa, $\nu_2 = 0.25$ and $E_3 = 0$. The volume fractions f_2 and f_3 hold such that $f_2 = 0.173(1 - f_3)$ according to Cohen and Ishai (1967). It is seen from Fig. 1(a) that the predictions given by the present method (coupled and decoupled) agree well with those of Huang et al. (1994) calculated using the decoupled formulas Eqs. (7) and (8) together with the GSCM predictions of Christensen and Lo (1979) for two-phase composites. All the theoretical predictions agree well with the experimental data of Cohen and Ishai (1967). The Mori-Tanaka prediction (Weng, 1984) deviates from the experimental data slightly for high void volume fractions.

In order to further examine the accuracy of the present scheme, we next consider a composite containing two kinds of inhomogeneity with extreme stiffnesses: the first kind is rigid particles ($E_2 = \infty$) and the second is void ($E_3 = 0$). The Poisson ratio of the matrix is taken as 0.3. The voids weaken the composite, while the rigid particles stiffen it. Fig. 1(b) shows the competition between the voids and the rigid inhomogeneities. Previously, Molinari and El Mouden (1996) presented a cluster model which needs some numerical computation but is generally better than the MTM in taking into account the inhomogeneity interactions to predict the effective moduli of composites. Fig. 1(b) also compares the results obtained by the present scheme (coupled and decoupled) with the numerical results of Molinari and El Mouden (1996) for this three-phase composite, and the comparison shows that these two methods are very close. It is interesting to note that, for a material containing equal amounts of voids and rigid inhomogeneities, the Young's modulus almost retains the value of the matrix material, as found by Huang et al. (1994).

3.2. Fibre-reinforced composites

Likewise, for aligned fibre-reinforced composites, Huang et al. (1994) also proposed the following decoupled formulas to calculate the effective transverse plane-strain bulk modulus and the effective transverse shear modulus:

$$\frac{\bar{k}}{k_1} \cong \prod_{I=2}^{N} \frac{\bar{k}_0}{k_1}\left(f_I, \frac{\mu_{TI}}{\mu_1}, \nu_I, \nu_1\right) \tag{9}$$

$$\frac{\bar{\mu}_T}{\mu_1} \cong \prod_{I=2}^{N} \frac{\bar{\mu}_{T0}}{\mu_1}\left(f_I, \frac{\mu_{TI}}{\mu_1}, \nu_I, \nu_1\right) \tag{10}$$

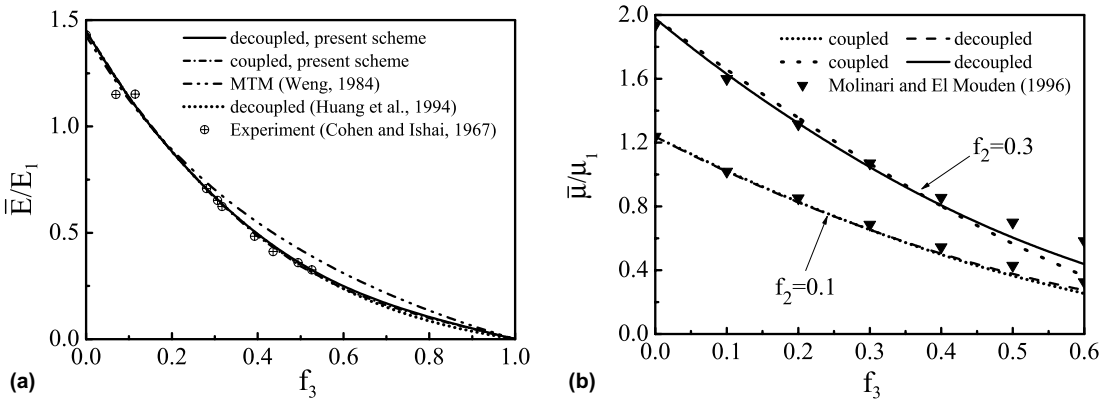

Fig. 1. Comparison of the present scheme (coupled and decoupled) with Huang et al. (1994, decoupled), MTM (Weng, 1984) and experimental results (Cohen and Ishai, 1967) for a composite comprising epoxy, quartz sand particles and voids (a). Comparison of the present scheme (coupled and decoupled) with the predictions of Molinari and El Mouden (1996) for a composite containing rigid particles and voids (b).

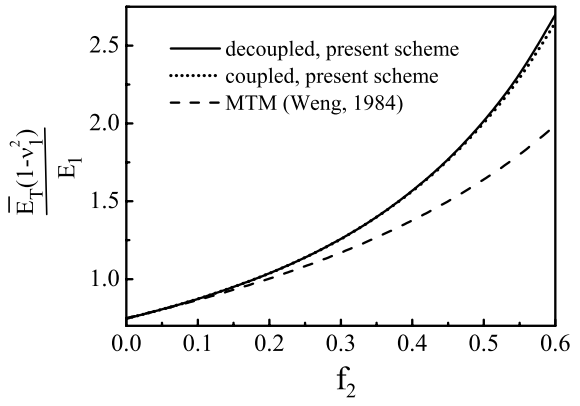

Fig. 2. Comparison of the present scheme (coupled and decoupled) with MTM (Weng, 1984) for a fibre-reinforced composite.

where $\bar{k}_0$ and $\bar{\mu}_{T0}$ are the plane-strain bulk modulus and shear modulus of a two-phase composite containing only the I-th kind of fibre with the volume fraction f_I. Thus, $\bar{k}_0$ and $\bar{\mu}_{T0}$ are calculated from Eqs. (4) and (5). Our numerical results also show that the decoupled formulas in Eqs. (9) and (10) are very accurate compared with the numerical results computed from the nonlinear coupled algebraic equations. Fig. 2 shows the effective transverse plane-strain Young's modulus $\overline{E}_T$ of a three-phase composite obtained by the present scheme (coupled and decoupled), and the MTM (Weng, 1984), where $\overline{E}_T = 4\bar{k}\bar{\mu}_T/(\bar{k}+\bar{\mu}_T)$. The considered material is a boron fibre-reinforced composite with cylindrical voids. The material parameters are: $E_2/E_1 = 120.12$, $\nu_1 = 0.35$, $\nu_2 = 0.2$, $E_3/E_1 = 0$. The volume fraction of the voids is fixed at $f_3 = 0.1$. Fig. 2 shows that the results given by the decoupled formulas are practical the same as those by the numerical solutions of the coupled equations. It is seen that the MTM significantly underestimates the effective modulus compared with the GSCM. This feature is similar to what was found by Segurado and LLorca (2002) for composites reinforced by spherical particles.

4. Effective moduli of multiphase composites with interface effects

The effective moduli of multiphase particle-reinforced composites with the interface effects can be obtained easily by combining the expressions in Eqs. (1) and (2) for the effective moduli of two-phase composites, the elastic moduli of the equivalent particles in Eqs. (I16)–(I22) with the decoupled formulas in Eqs. (7) and (8); and those of the multiphase fibre-reinforced composites can be obtained by combining the formulas in Eqs. (4) and (5), the elastic moduli of the equivalent fibres in Eqs. (I26)–(I27), (I31)–(I32) and (I36)–(I37) with the decoupled formulas in Eqs. (9) and (10). Other elastic constants of the unidirectional fibre-reinforced composites can be calculated using the composite cylinder model. In the following, we will focus on the effective moduli of multiphase composites containing spherical inhomogeneities with various interface effects.

First, we predict the effective moduli of a four-phase particle-reinforced composite, with a matrix of epoxy, perfectly-bonded quartz-sand particles (second phase, volume fraction f_2), quartz-sand with free sliding interface (third phase, volume fraction f_3) and voids (fourth phase, volume fraction f_4). The material parameters of the epoxy matrix and quartz-sand are the same as those in Fig. 1(a); the quartz-sand particles with the free sliding interface can be equivalent to perfectly-bonded particles with the moduli given by Eqs. (I16)–(I17), but setting $m_r \to \infty$ and $m_\theta = 0$. In order to manifest the influence of the voids and the free-sliding bonding condition, we compare the effective moduli of the composites with and without these two factors. In the former case, $f_3 = f_4 = 0$, and in the latter $f_3 = f_4 = 0.1$. The numerical results for the two cases predicted using the present scheme and the MTM are shown in Fig. 3(a) and (b). These results are obtained under the condition $f_1 + f_2 + f_3 + f_4 = 1$. It is seen that the existence of the free sliding particles and voids can considerably decrease the effective moduli of the composite. The effective bulk modulus of the four-phase composite predicted by the present scheme is higher than that predicted by the MTM, whereas the effective shear modulus of the four-phase composite predicted by present scheme is lower than that by the MTM.

Next, we predict the effective moduli of a three-phase composite with an interphase. The matrix is cement paste with $\kappa_1 = 22.51$ GPa, $\mu_1 = 11.8$ GPa; the second phase is sand with $\kappa_2 = 44$ GPa, $\mu_2 = 37$ GPa; and the third phase is voids with $\kappa_3 = 0$, $\mu_3 = 0$. There is an interphase around the second phase (sand) with the elastic constants $\mu_c/\mu_2 = 0.50$, $\nu_c = 0.40$ and interphase thickness $t = 0.0588R_I$. These material parameters are taken from the work of Hashin and Monteiro (2002). The sand particles with the interphase can be equivalent to perfectly-bonded particles with the moduli

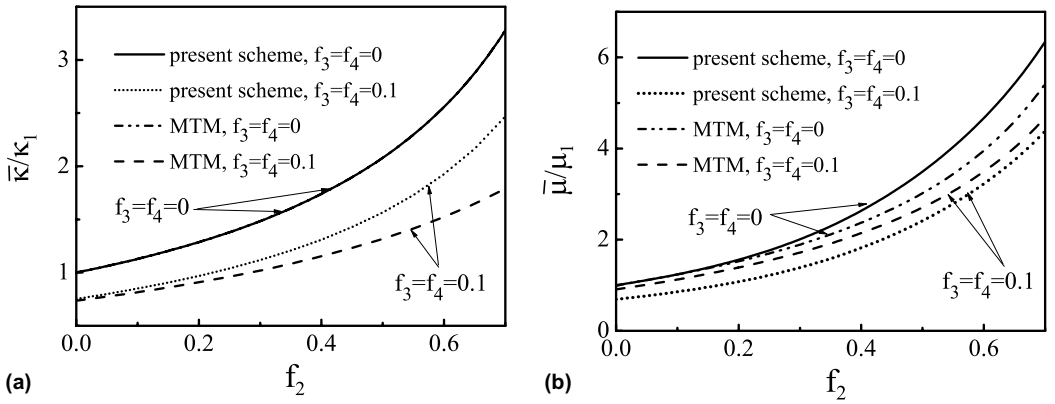

Fig. 3. Effective bulk modulus (a) and shear modulus (b) of a composite with perfectly-bonded particles, free-sliding particles and voids.

given by Eqs. (I21)–(I22). In order to manifest the influence of the voids, we compare the effective moduli when $f_3 = 0$ with those when $f_3 = 0.1$. The numerical results for the two cases predicted using the present scheme and the MTM are given in Fig. 4(a) and (b). It is seen that the bulk and shear moduli predicted by the present scheme are slightly higher than those predicted by the MTM for the three-phase composite ($f_3 = 0.1$). However, for the two-phase composite ($f_3 = 0$), the bulk modulus predicted by the present scheme is equal to that by the MTM, and the shear modulus predicted by the present scheme is almost the same as that by the MTM.

5. Scaling laws for size-dependence

It can be seen from Section 3.2 and 3.3 of Part I that when the linear-spring model and the interface stress model are considered, some intrinsic length scales emerge. These length scales are

$$l_r = \frac{\mu_1}{\alpha_n}, \quad l_\theta = \frac{\mu_1}{\alpha_s}, \quad \text{for the linear-spring model} \tag{11}$$

$$l_\lambda = \frac{\lambda_s}{\mu_1}, \quad l_\mu = \frac{\mu_s}{\mu_1}, \quad \text{for the interface stress model} \tag{12}$$

Therefore, by dimensional analysis, the non-dimensional effective moduli of the composites with these interface effects will generally depend upon the size of the particles or fibres. This size-dependence is important for the characterization of composites and polycrystalline materials. The detailed size-dependence of the effective moduli can be studied following the above micromechanical scheme. However, as will be shown below, when the length scales are small compared with the characteristic size of the composites, the size-dependence can be depicted concisely and accurately by two simple scaling laws. For the purpose of illustration, we only consider

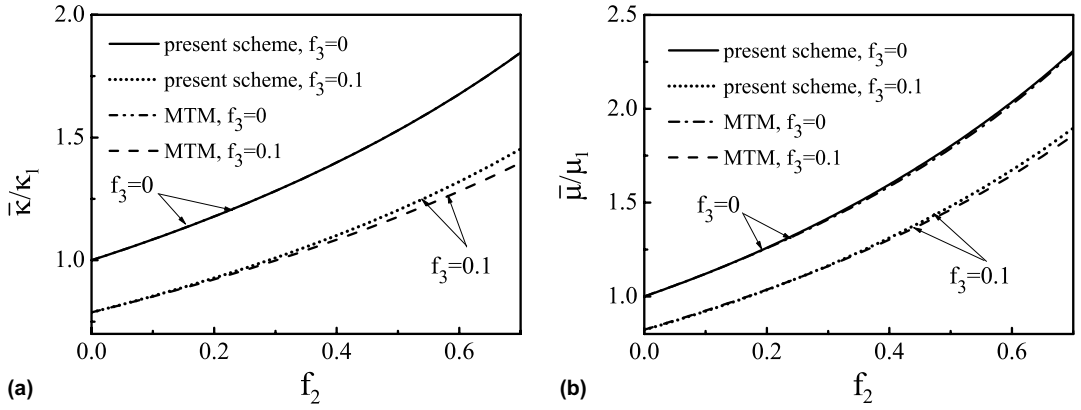

Fig. 4. Effective bulk modulus (a) and shear modulus (b) of a composite containing spherical particles with an interphase and spherical voids.

two-phase composites. The size-dependence of the effective moduli of multiphase composites with the interface effects also obeys the similar scaling laws.

5.1. Scaling law for linear-spring interface model

For the linear-spring interface model, as is shown above, there are two intrinsic length scales l_r and l_θ. Thus, the non-dimensional effective moduli of the composite can be expressed as the functions of the non-dimensional parameters l_r/L and l_θ/L, where L denotes the radius of the spherical particles or the radius of the cylindrical fibres. We can then expand the functions into Taylor series of the variables l_r/L and l_θ/L. When these variables are small such that the terms of the order two and higher can be neglected and only the linear terms are retained, these functions can then be expressed in a simple form as follows:

$$\frac{H(\infty)}{H(L)} = 1 + \frac{1}{L}(\Upsilon_r l_r + \Upsilon_\theta l_\theta) \tag{13}$$

where Υ_r and Υ_θ are two non-dimensional parameters. $H(L)$ denotes the property corresponding to a characteristic size L, say, the radius of the particles, and $H(\infty)$ denotes the same property when $L \to \infty$ or, equivalently, when the interface effect is vanishingly small. Previously, Nan et al. (1998) used the tangential linear-spring model to simulate the elastic behaviour of nanocrystals, and obtained a simple scaling law similar to that in Eq. (13). In their scaling law, there is only one intrinsic length scale.

After some algebraic manipulations, it can be shown that for composites reinforced by spherical particles with the linear-spring interface effect, the scaling laws for the effective elastic constants of the composites are

$$\frac{\bar{\kappa}(\infty)}{\bar{\kappa}(R_I)} = 1 + \frac{3f_I\kappa_I^2(3\kappa_1+4\mu_1)^2}{G_1\mu_1}\frac{l_r}{R_I} \tag{14}$$

$$\frac{\bar{\mu}(\infty)}{\bar{\mu}(R_I)} = 1 + \frac{90f_I g_3^2(1-\nu_1)^2}{G_2}\frac{(2l_r+3l_\theta)}{R_I} \tag{15}$$

in which

$$G_1 = [4(1-f_I)\kappa_1\mu_1 + \kappa_I(3\kappa_1+4f_I\mu_1)] \times [3(1-f_I)\kappa_I + 3f_I\kappa_1 + 4\mu_1] \tag{16}$$

$$G_2 = 4(1+f_I)(28-45\nu_1)g_3 + \frac{12}{5}(2+f_I-3f_I^2)(5-9\nu_1)g_3^2 + (5-2f_I-3f_I^2)(7-5\nu_1) \tag{17}$$

For unidirectional fibre-reinforced composites with the linear-spring interface effect, the scaling law for the effective elastic constants are

$$\frac{\bar{k}(\infty)}{\bar{k}(\rho_I)} = 1 + \frac{2f_Ik_I^2(k_1+\mu_1)^2}{\mu_1[(1-f_I)k_I+f_Ik_1+\mu_1][(1-f_I)k_1\mu_1+k_I(k_1+f_I\mu_1)]} \times \frac{l_r}{\rho_I} \tag{18}$$

$$\frac{\bar{\mu}_{\mathrm{T}}(\infty)}{\bar{\mu}_{\mathrm{T}}(\rho_I)} = 1 + \frac{16f_Ig_2^2(1-\nu_1)^2}{G_3}\frac{(l_r+l_\theta)}{\rho_I} \tag{19}$$

$$\frac{\bar{\mu}_{\mathrm{L}}(\infty)}{\bar{\mu}_{\mathrm{L}}(\rho_I)} = 1 + \frac{4f_I\mu_I^2}{(1-f_I^2)(\mu_I^2+\mu_1^2)+2(1+f_I^2)\mu_I\mu_1}\frac{l_\theta}{\rho_I} \tag{20}$$

in which

$$G_3 = 3(1+f_I^2)g_2 + 3(1-f_I)g_2^2(3+f_I-5\nu_1) \times (1-\nu_1) + (1-f_I)(1+2f_I-3f_I\nu_1) \tag{21}$$

In Eqs. (18) and (19), $\bar{k}$ denotes the effective transverse plane-strain bulk modulus, $\bar{\mu}_{\mathrm{T}}$ denotes the transverse shear modulus, and $\bar{\mu}_{\mathrm{L}}$ the longitudinal shear modulus.

The other two elastic constants related to the fibre direction, namely, the longitudinal Poisson ratio $\bar{\nu}_{\mathrm{L}}$ and the longitudinal Young modulus $\bar{E}_{\mathrm{L}}$, are nearly unaffected by the interface effect

$$\frac{\bar{\nu}_{\mathrm{L}}(\infty)}{\bar{\nu}_{\mathrm{L}}(\rho_I)} \approx 1 \tag{22}$$

$$\frac{\bar{E}_{\mathrm{L}}(\infty)}{\bar{E}_{\mathrm{L}}(\rho_I)} \approx 1 \tag{23}$$

By comparing the predictions of these scaling laws with those calculated using the formulas in the micromechanical scheme, it can be verified that when $l_r \leqslant 0.05R_I(\rho_I)$ and $l_\theta \leqslant 0.05R_I(\rho_I)$, the scaling laws are very accurate.

It is interesting to note that as G_1 and G_2 are always positive for $f_I \leqslant 1.0$ and $\nu_1 \leqslant 0.5$, the coefficients of l_r/R_I and l_θ/R_I in the second terms on the right hand sides of Eqs. (14) and (15) will be positive. Therefore, the effective moduli will decrease with the decrease of the size of the particles for the same volume fraction f_I. For nanocrystalline materials in which the grain boundary has a lower elastic modulus than those of the grains (e.g. Kluge et al., 1990; Zhang and Hack, 1992), Schiøtz et al. (1998) indicated that most of the deformation occurs in the grain boundary region, and in the linear elastic region the Young modulus of the nanocrystalline material decreases with the decrease of

the size of the grains. Therefore, the size-dependence of the elastic behaviour of the nanocrytsalline material is qualitatively in accordance with what is predicted by the scaling laws in Eqs. (14) and (15).

5.2. Scaling law for interface stress model

As mentioned in Part I, the effect of the surface/interface stress on the mechanical behaviour of materials has intensified recently for its importance in the properties of nano-structured materials (e.g. Cuenot et al., 2004; Duan et al., 2005a,b,c; Shenoy, 2005; Dingreville et al., 2005). The property of an isotropic interface is characterized by two interface elastic constants λ_s and μ_s, giving rise to two intrinsic length scales l_λ and l_μ in Eq. (12). Duan et al. (2005a) predicted the effective elastic moduli of heterogeneous solids containing spherical inhomogeneities with the interface stress effect using the composite sphere model, the Mori-Tanaka method, and the coventional generalized self-consistent method. In addition, Duan et al. (2005b) presented the Eshelby and stress concentration tensors for a spherical inhomogeneity embedded in an infinite medium with the interface stress effect. The salient features of these tensors are their position- and size-dependence. Therefore, Duan et al. (2005a,b), Wang et al. (2006) pointed out that the size-dependence of the effective moduli, and the Eshelby and stress concentration tensors can be depicted by the following scaling laws:

$$\frac{H(L)}{H(\infty)} = 1 + \frac{1}{L}(\Upsilon_\lambda l_\lambda + \Upsilon_\mu l_\mu) \tag{24}$$

Here, Υ_λ and Υ_μ are two non-dimensional parameters, $H(L)$ is the property corresponding to a characteristic size L, and $H(\infty)$ denotes the property when $L \to \infty$ or, equivalently, when the interface effect is vanishingly small. In fact, Wang et al. (2006) have found that many properties of nano-structured materials obey the scaling law in Eq. (24).

For composites reinforced by spherical particles with the interface stress effect, the scaling laws for the effective moduli are

$$\frac{\bar{\kappa}(R_I)}{\bar{\kappa}(\infty)} = 1 + \frac{4\mu_1(3\kappa_1 + 4f_I\mu_1)}{4(1-f_I)\kappa_1\mu_1 + \kappa_I(3\kappa_1 + 4f_I\mu_1)} \frac{(l_\lambda + l_\mu)}{3R_I} \tag{25}$$

$$\frac{\bar{\mu}(R_I)}{\bar{\mu}(\infty)} = 1 + \frac{45f_I(1-\nu_1)^2}{M[M - 15f_I(1-g_3)(1-\nu_1)]} \frac{(l_\lambda + 7l_\mu)}{R_I} \tag{26}$$

in which

$$M = 7 + 8f_I - 5(1+2f_I)\nu_1 + 2(1-f_I)(4-5\nu_1)g_3 \tag{27}$$

For the fibre-reinforced composites, the scaling law for the effective moduli are

$$\frac{\bar{k}(\rho_I)}{\bar{k}(\infty)} = 1 + \frac{\mu_1(k_1 + f_I\mu_1)}{(1-f_I)k_1\mu_1 + k_I(k_1 + f_I\mu_1)} \frac{(l_\lambda + 2l_\mu)}{2\rho_I} \tag{28}$$

$$\frac{\bar{\mu}_{\mathrm{T}}(\rho_I)}{\bar{\mu}_{\mathrm{T}}(\infty)} = 1 + \frac{4f_I(1-\nu_1)^2}{N} \frac{(l_\lambda + 2l_\mu)}{\rho_I} \tag{29}$$

$$\frac{\bar{\mu}_{\mathrm{L}}(\rho_I)}{\bar{\mu}_{\mathrm{L}}(\infty)} = 1 + \frac{(1+f_I)\mu_1}{(1+f_I)\mu_{LI} + (1-f_I)\mu_1} \frac{l_\mu}{\rho_I} \tag{30}$$

in which

$$N = [1 + 3f_I - 4f_I\nu_1 + (1-f_I)(3-4\nu_1)g_2] \times [1 - f_I + (3 + f_I - 4\nu_1)g_2] \tag{31}$$

Similar to the linear-spring interface model, the longitudinal Poisson ratio $\bar{\nu}_{\mathrm{L}}$ and the longitudinal Young modulus $\overline{E}_{\mathrm{L}}$ are nearly unaffected by the interface effect

$$\frac{\bar{\nu}_{\mathrm{L}}(\rho_I)}{\bar{\nu}_{\mathrm{L}}(\infty)} \approx 1 \tag{32}$$

$$\frac{\overline{E}_{\mathrm{L}}(\rho_I)}{\overline{E}_{\mathrm{L}}(\infty)} \approx 1 \tag{33}$$

It can be verified that the scaling laws are very accurate when $l_\lambda \leqslant 0.1R_I(\rho_I)$ and $l_\mu \leqslant 0.1R_I(\rho_I)$.

It is noted that previously, Miller and Shenoy (2000), and Shenoy (2002), in studying the elastic constants of monolithic nanobeams and nanoplates taking into account the surface stress effect, have presented a scaling law $H(L)/H(\infty) = 1 + \alpha l_{in}/L$, where l_{in} is the ratio of the surface elastic modulus to the Young modulus of the bulk material, and α is a non-dimensional parameter.

5.3. Additional remarks

We recall that the linear-spring interface model can be used to approximate a thin and soft interphase (Hashin, 2002; Wang et al., 2005), and an imperfect interface (Tan et al., 2005), whereas the interface stress model can be used to approximate a thin and stiff interphase (Wang et al., 2005), and the excess bulk stress at an interface (Müller and Saúl, 2004). For the linear-spring model, the traction across the interface is continuous but the displacement is discontinuous, whereas for the interface stress model, the traction is discontinuous

across the interface but the displacement is continuous. Therefore, these two interface models possess a sort of symmetry from a physical point of view. Interestingly, as the left hand sides of the scaling laws in Eqs. (13) and (24) are formally inverse of each other, the two scaling laws depicting these two interface effects also possess a sort of symmetry from a mathematical point of view.

6. Conclusions

In terms of the replacement procedure developed Part I, spherical particles and fibres with the interface effects can be replaced by equivalent homogeneous particles and fibres, respectively. These equivalent particles and fibres are then embedded in the respective matrix materials of the composites, where the conventional continuous conditions prevail at the interfaces. Thus, the problems with the interface effects are converted into those without any interface effects. Therefore, in this part of the two-part paper, the expressions for the effective moduli of composites containing perfectly bonded particles and fibres are given using the generalized self-consistent prediction based upon the Eshelby equivalent inclusion method in an average sense for the three-phase configuration. It is shown that these expressions are very accurate but much simpler than those predicted using the classical generalized self-consistent method. The influence of the interfacial bonding conditions on the effective moduli of composites are examined, and it is shown that the interfacial bonding condition can considerably affect the stiffening effect of the particles. When the linear-spring and interface stress effects are taken into account, some intrinsic length scales emerge and thus the effective moduli of the composites become dependent upon the size of the particles and fibres. The general size-dependence can be easily studied following the procedure of the developed micromechanical scheme. However, it is shown that when the ratios of the intrinsic length scales to the size of the particles/fibres are small, the size-dependence can be depicted accurately by two simple scaling laws.

Acknowledgements

This work is supported by the National Natural Science Foundation of China under Grant No. 10525209 and 10372004.

References

Benveniste, Y., 1987. A new approach to the application of Mori-Tanaka's theory in composite materials. Mech. Mater. 6, 147–157.

Christensen, R.M., Lo, K.H., 1979. Solutions for effective shear properties in three phase sphere and cylinder models. J. Mech. Phys. Solids 27, 315–330.

Cohen, L.J., Ishai, O., 1967. The elastic properties of three-phase composites. J. Compos. Mater. 1, 390–396.

Cuenot, S., Frétigny, C., Demoustier-Champagne, S., Nysten, B., 2004. Surface tension effect on the mechanical properties of nanomaterials measured by atomic force microscopy. Phys. Rev. B 69, 165410-1–165410-5.

Dingreville, R., Qu, J., Cherkaoui, M., 2005. Surface free energy and its effect on the elastic behaviour of nano-sized particles, wires and films. J. Mech. Phys. Solids 53, 1827–1854.

Duan, H.L., Wang, J., Huang, Z.P., Karihaloo, B.L., 2005a. Size-dependent effective elastic constants of solids containing nano-inhomogeneities with interface stress. J. Mech. Phys. Solids 53, 1574–1596.

Duan, H.L., Wang, J., Huang, Z.P., Karihaloo, B.L., 2005b. Eshelby formalism for nano-inhomogeneities. Proc. R. Soc. A 461, 3335–3353.

Duan, H.L., Wang, J., Huang, Z.P., Luo, Z.Y., 2005c. Stress concentration tensors of inhomogeneities with interface effects. Mech. Mater. 37, 723–736.

Duan, H.L., Jiao, Y., Yi, X., Huang, Z.P., Wang, J. Solutions of inhomogeneity problems with graded shells and application to core-shell nanoparticles and composites. J. Mech. Phys. Solids, in press.

Hashin, Z., 1966. Viscoelastic fiber reinforced materials. AIAA J. 4, 1411–1417.

Hashin, Z., 2002. The interphase/imperfect interface in elasticity with application to coated fiber composites. J. Mech. Phys. Solids 50, 2509–2537.

Hashin, Z., Monteiro, P.J.M., 2002. An inverse method to determine the elastic properties of the interphase between the aggregate and the cement paste. Cement Concrete Res. 32, 1291–1300.

Hill, R., 1964. Theory of mechanical properties of fibre-strengthened materials: elastic behaviour. J. Mech. Phys. Solids 12, 199–212.

Huang, Y., Hu, K.X., Wei, X., Chandra, A., 1994. A generalized self-consistent mechanics method for composite materials with multiphase inclusions. J. Mech. Phys. Solids 42, 491–504.

Kluge, M.D., Wolf, D., Lutsko, J.F., Phillpot, S.R., 1990. Formalism for the calculation of local elastic constants at grain boundaries by means of atomistic simulation. J. Appl. Phys. 67, 2370–2379.

Miller, R.E., Shenoy, V.B., 2000. Size-dependent elastic properties of nanosized structural elements. Nanotechnology 11, 139–147.

Molinari, A., El Mouden, M., 1996. The problem of elastic inclusions at finite concentration. Int. J. Solids Struct. 33, 3131–3150.

Mori, T., Tanaka, K., 1973. Average stress in matrix and average elastic energy of materials with misfitting inclusions. Acta Metall. 21, 571–574.

Müller, P., Saúl, A., 2004. Elastic effects on surface physics. Surf. Sci. Rep. 54, 157–258.

Nan, C.W., Li, X.P., Cai, K.F., Tong, J.Z., 1998. Grain size-dependent elastic moduli of nanocrystals. J. Mater. Sci. Lett. 17, 1917–1919.

Schiøtz, J., Di Tolla, F.D., Jacobsen, K.W., 1998. Softening of nanocrystalline metals at very small grain sizes. Nature 391, 561–563.

Segurado, J., LLorca, J., 2002. A numerical approximation to the elastic properties of sphere-reinforced composites. J. Mech. Phys. Solids 50, 2107–2121.

Shenoy, V.B., 2002. Size-dependent rigidities of nanosized torsional elements. Int. J. Solids Struct. 39, 4039–4052.

Shenoy, V.B., 2005. Atomistic calculations of elastic properties of metallic fcc crystal surfaces. Phys. Rev. B 71, 094104-1–094104-11.

Tan, H., Liu, C., Huang, Y., Geubelle, P.H., 2005. The cohesive law for the particle/matrix interfaces in high explosives. J. Mech. Phys. Solids 53, 1892–1917.

Wang, J., Duan, H.L., Zhang, Z., Huang, Z.P., 2005. An anti-interpenetration model and connections between interphase and interface models in particle-reinforced composites. Int. J. Mech. Sci. 47, 701–708.

Wang, J., Duan, H.L., Huang, Z.P., Karihaloo, B.L., 2006. A scaling law for properties of nano-structured materials. Proc. R. Soc. A 462, 1355–1363.

Weng, G.J., 1984. Some elastic properties of reinforced solids, with special reference to isotropic ones containing spherical inclusions. Int. J. Eng. Sci. 22, 845–856.

Zhang, T.-Y., Hack, J.E., 1992. On the elastic stiffness of grain boundaries. Phys. Stat. Sol. (a) 131, 437–443.